

# REPORT DOCUMENTATION PAGE

Form Approved  
OMB No. 0704-0188

Public reporting burden for this collection of information is estimated to average 1 hour per response, including the time for reviewing instructions, searching existing data sources, gathering and maintaining the data needed, and completing and reviewing this collection of information. Send comments regarding this burden estimate or any other aspect of this collection of information, including suggestions for reducing this burden to Department of Defense, Washington Headquarters Services, Directorate for Information Operations and Reports (0704-0188), 1215 Jefferson Davis Highway, Suite 1204, Arlington, VA 22202-4302. Respondents should be aware that notwithstanding any other provision of law, no person shall be subject to any penalty for failing to comply with a collection of information if it does not display a currently valid OMB control number. PLEASE DO NOT RETURN YOUR FORM TO THE ABOVE ADDRESS.

1. REPORT DATE (DD-MM-YYYY) 07-01-2000	2. REPORT TYPE Paper	3. DATES COVERED (From - To)		
4. TITLE AND SUBTITLE  <b>Simultaneous Whole-Field Measurements of Velocity and Concentration Fields Using Combined MTV and LIF</b>		5a. CONTRACT NUMBER		
		5b. GRANT NUMBER		
		5c. PROGRAM ELEMENT NUMBER		
6. AUTHOR(S)  M.M. Koochesfahani; <sup>1</sup> R.K. Cohn; <sup>2</sup> C.G. MacKinnon*		5d. PROJECT NUMBER		
		5e. TASK NUMBER		
		5f. WORK UNIT NUMBER		
7. PERFORMING ORGANIZATION NAME(S) AND ADDRESS(ES) AND ADDRESS(ES)  <sup>1</sup> Department of Mechanical Engineering Michigan State University East Lansing, MI 48824		8. PERFORMING ORGANIZATION REPORT  <sup>2</sup> Air Force Research Laboratory (AFMC) AFRL/PRS 5 Pollux Drive Edwards AFB CA 93524-7048		
*Currently at Daimler-Chrysler, MI				
9. SPONSORING / MONITORING AGENCY NAME(S) AND ADDRESS(ES)  Air Force Research Laboratory (AFMC) AFRL/PRS 5 Pollux Drive Edwards AFB CA 93524-7048		10. SPONSOR/MONITOR'S ACRONYM(S)		
		11. SPONSOR/MONITOR'S NUMBER(S) AFRL-PR-ED-TP-2000-006		
12. DISTRIBUTION / AVAILABILITY STATEMENT Approved for public release; distribution unlimited.				
13. SUPPLEMENTARY NOTES				
14. ABSTRACT				
15. SUBJECT TERMS				
16. SECURITY CLASSIFICATION OF:  a. REPORT Unclassified		17. LIMITATION OF ABSTRACT  A	18. NUMBER OF PAGES	19a. NAME OF RESPONSIBLE PERSON Jay Levine
b. ABSTRACT Unclassified				19b. TELEPHONE NUMBER (include area code) (661) 275-6179
c. THIS PAGE Unclassified				

20020115 095

# Simultaneous Whole-Field Measurements of Velocity and Concentration Fields Using Combined MTV and LIF

Manoochehr Koochesfahani, Richard Cohn\*, and Colin MacKinnon†

Department of Mechanical Engineering  
Michigan State University  
East Lansing, MI 48824

## Abstract

A new technique is described for the simultaneous measurement of velocity and concentration fields. We describe here applications in liquid-phase flows, but the methodology can be extended to gas-phase flows with appropriate tracers. In this single-laser, two-tracer approach, molecular tagging velocimetry (MTV) based on a phosphorescent compound is combined with laser induced fluorescence (LIF) using fluorescein as tracer. Results show that one can design experiments with minimal cross-talk between the LIF and MTV signals. Application of the simultaneous MTV-LIF technique is demonstrated by performing simultaneous flow visualization and vorticity measurements in a low Reynolds number forced wake and simultaneous velocity-concentration measurements in a turbulent mixing layer. Preliminary data are presented on the mean and rms fluctuation of velocity and concentration, along with the correlation between velocity and concentration fluctuations.

---

\* Currently at AFRL/PRSA, 10 E. Saturn Blvd, Edwards Air Force Base, CA 93524.

† Currently at Daimler-Chrysler, Michigan.

## 1. Introduction

Simultaneous information on a passive scalar and the velocity field is desirable in many fluid flow investigations. In turbulent mixing applications, the species concentration field  $\xi$  is determined by molecular diffusion and transport by the turbulent flow field. When considering the Reynolds-averaged scalar conservation equation, the effects of turbulent transport appear in terms of the correlation between the concentration and velocity fluctuations, i.e. expressions such as  $\overline{u' \xi'}$  and  $\overline{v' \xi'}$ . Experimental characterization of these correlations is needed for the development and validation of physical models, and this requires the simultaneous measurement of the velocity and concentration fields.

Scalar quantities, such as tracer concentration or temperature, are also often used to visualize flow patterns and infer general flow structures. A good example is the use of fluorescent tracers along with laser induced fluorescence (LIF) for visualization of liquid and gas phase flows. LIF images are routinely used to make inferences about the vortical structures and their dynamics in various flows, even though it is known that such inferences can sometimes be misleading. The ability to simultaneously visualize the flow structure and measure its underlying velocity/vorticity field would serve as a valuable tool in discovering and understanding flow physics.

There exists an extensive body of literature on the measurements of *either* velocity components *or* scalar quantities (e.g. temperature, concentration) in many types of flows. Studies involving simultaneous velocity and scalar measurements are far more limited. One of the earliest was the study of a helium jet by Keagy & Weller (1949) where they measured the profiles of mean velocity using a Pitot probe and mean concentration using a sampling probe. Way & Libby (1970, 1971), following a suggestion from Corrsin, developed a two-sensor hot-wire probe capable of monitoring fluctuations of both one velocity component and concentration in a low-speed helium jet. Antonia et al. (1975) and Chevray & Tutu (1978) produced results involving two fluctuating velocity components and temperature fluctuations using a cold-wire sensor mounted on an X-wire probe in heated air jets. The investigations mentioned above provide examples of work relying on intrusive probes.

More recently, the advent of optical diagnostics such as LDV, LIF and particle scattering techniques have presented new opportunities for the non-intrusive simultaneous acquisition of multiple flow variables. Owen (1976) used a combination of LDV and LIF to measure velocity and concentration correlations in a co-axial liquid jet. Stärner (1983) and Dibble & Schefer (1983) acquired velocity, density, and species concentration via LDV/Mie scattering and LDV/Raman scattering, respectively, in a diffusion flame. Similar to the earlier work of Owen, Lemoine et al. (1996) obtained simultaneous velocity and concentration data using LDV and LIF in a co-flowing

liquid jet. All of the above investigations, however, have incorporated single point measurements.

Whole-field velocimetry techniques such as particle image velocimetry (PIV), and its digital counterpart (DPIV), have lead to recent efforts for obtaining planar measurements of velocity and concentration or temperature. Simultaneous planar measurements have been reported by Frank et al. (1996), and O'Hern et al. (1999), who combined PIV and LIF to record two velocity components as well as concentration in gas-phase flows. Such combined measurements have also been reported in liquid phase flows (e.g. see Cowen & Chang, 1999; Law & Wang, 1999; Webster et al., 1999). For simultaneous velocity-temperature measurements in liquids, use has been made of liquid crystal encapsulate microspheres (e.g. Ozawa et al., 1992 and Dabiri & Gharib, 1996), or combining PIV and LIF while taking advantage of the temperature dependence of fluorescence emission (see Hishida & Sakakibara, 1999 and Grissino et al., 1999).

Since the optical velocimetry techniques mentioned above rely on scattering from seed particles, the potential artifacts connected to the use of seed particles need to be evaluated for each experiment. Some of these artifacts are related to flow tracking issues (i.e. particle size, density mismatch). Even if particles track the flow perfectly, strong out-of-plane motions that bring particles in and out of the laser sheet can affect the accuracy of in-plane velocity measurements in PIV. When combined with LIF, additional complications need to be carefully considered such as the influence of laser light absorption and scattering by the seed particles on the LIF signal.

Various approaches have been advanced recently to obtain the fluid velocity field directly from the images of the scalar field either through the use of the passive scalar conservation equation itself (Dahm et al., 1992; Pearlstein & Carpenter, 1995) or the correlation of features in the scalar field (Maas et al., 1994; Tokumaru & Dimotakis, 1995). The determination of the velocity field (even 2 components of the velocity over a plane) requires instantaneous volumetric concentration data, which has usually been obtained using planar LIF measurements and scanning the plane of the laser sheet through the volume of interest. The resulting high-speed scanning requirements, and the corresponding high-speed, high framing rate imaging needs, have so far limited these approaches to very slow flow speeds (on the order of a few mm/s). In addition, velocity information can only be obtained in the regions of the flow where the scalar field has sufficient gradients. In particular, there is no velocity information where the concentration is uniform (e.g. in free streams or in regions within a turbulent flow where free stream fluids have been entrained.). For the most general case, it is preferable to decouple the velocity measurement from the scalar field measurement, as we describe in this paper.

The present work combines Molecular Tagging Velocimetry (MTV) with LIF for the simultaneous planar measurements of velocity and concentration fields. One advantage of the

molecular tagging approach is that issues such as the tracking of the flow by the seed particles are eliminated. Also because of its molecular nature, MTV naturally lends itself to being combined with other molecular techniques such as LIF. The presentation here first gives a brief introduction to the MTV technique, followed by the methodology for simultaneous velocity-concentration measurements. Examples of the application of this diagnostic technique are given first in a low Reynolds number forced wake, where simultaneous flow visualization and vorticity data are provided. Then, preliminary data on the velocity-concentration correlations in a turbulent two-stream shear layer are discussed. Early aspects of this work have been previously presented in Koochesfahani & MacKinnon (1998 a,b).

## 2. Molecular Tagging Velocimetry

This method of velocimetry relies on molecules that can be turned into long lifetime tracers upon excitation by photons of an appropriate wavelength. Typically a pulsed laser is used to "tag" the regions of interest, and those tagged regions are interrogated at two successive times within the lifetime of the tracer. The measured Lagrangian displacement vector provides the estimate of the velocity vector. This technique can be thought of as the *molecular* counterpart of PIV, and offers advantages in situations where the use of seed particles is either not desirable or may lead to complications. This section provides only a brief description of the technique. A much more complete review, along with a more extensive list of related references, can be found in Koochesfahani (1999). Two earlier reviews (Falco & Nocera, 1993 and Koochesfahani et al., 1996) also contain relevant information on this topic.

The MTV technique has advanced significantly over the past decade in terms of the availability of new molecular tracers, methods of tagging, detection/imaging, and data processing. The application in liquid-phase flows, originally based on using photochromic molecules in organic solvents (Popovich & Hummel, 1967; Falco & Chu, 1987), has been expanded considerably by the availability of water-soluble compounds such as caged fluorescent molecules (Lempert et al., 1995) and engineered phosphorescent supramolecules (Gendrich et al., 1997). For gas-phase applications, techniques have been developed based on the use of excited-state oxygen (Miles et al., 1987, 1989), ozone O<sub>3</sub> (Pitz et al., 1996; Ribarov et al., 1999), OH (Wehrmeyer et al., 1999), and phosphorescent molecules such as biacetyl (Stier & Koochesfahani, 1999).

The work described here takes advantage of phosphorescent supramolecules, a new class of water-soluble compounds suitable for molecular tagging diagnostics. When a phosphorescent compound is used for molecular tagging, excitation by photons produces a long-lived excited state which is interrogated through its phosphorescence emission as the molecule radiatively returns to

its ground state. The long lifetime tracer is the excited state molecule itself. In this case only one source of photons is needed, the tagging process occurs during the laser pulse (a few nanoseconds in our case), and the excitation/emission process is reversible, which means the chemicals are reusable. The difficulty is that long-lived excited states (i.e. phosphorescence) suffer from  $O_2$  and  $H_2O$  quenching, and as a result, suitable molecular complexes have not been available until recently. New findings by Ponce et al. (1993) and Hartmann et al. (1996) have shown that supramolecules may be designed to exhibit long-lived phosphorescence which is not quenched. The design prevents the quenching of a lumophore by mixing certain alcohols (indicated collectively by "ROH") with an aqueous solution of a cyclodextrin (CD) "cup" that contains the lumophore. Cyclodextrins are molecules constructed from sugars connected in a head-to-tail arrangement forming a cup-shaped cavity. The CD used in the applications to date is G $\beta$ -CD, which is constructed of 7 glucose subunits with one additional glucose bonded to the rim of the cup to improve its solubility in water, the lumophore is 1-bromonaphthalene (1-BrNp) which absorbs efficiently at  $\lambda = 308$  nm, and the alcohol is typically cyclohexanol. The addition of alcohol forms a ternary complex (1-BrNp · G $\beta$ -CD · ROH), where the alcohol hydrogen bonds to the rim of the CD cup and acts as its lid, thereby shielding 1-BrNp from oxygen. (For this particular supramolecule the phosphorescence is not significantly quenched by  $H_2O$ .) The resulting long-lived, green phosphorescence has a typical lifetime  $\tau \approx 5$  ms. Further details of the properties of these compounds relevant to the MTV implementation and other applications are found in Gendrich, et al. (1997).

Past applications of MTV have considered the measurement of either one component or two components of the velocity vector over a plane. In order to unambiguously measure two components of the velocity in a plane, the luminescence intensity field from a tagged region must have spatial gradients in two, preferably orthogonal, directions. In our method of implementation, this is achieved by creating a grid of intersecting laser lines for the purpose of tagging. The grid of laser lines is generated from the main beam of an excimer laser using standard optics (cylindrical and spherical optics, beam splitter and beam blockers); see Gendrich et al. (1997) for details. Figure 1 shows an example of a region tagged by a grid pattern. This example, taken from a water study of the flow field of a vortex ring impacting a solid wall at normal incidence, shows both the initially tagged regions and their subsequent evolution after a time delay, along with the resultant velocity vector field derived from this image pair using a spatial correlation method (see later discussion).

The MTV image pairs are acquired by a pair of CCD detectors which view the same region of interest in the flow through a cube beam splitter. Immediately after the pulsed laser fires, the first detector records an initial image of the tagged regions. After a prescribed time delay  $\Delta t$ , the

second detector records a second image of the tagged regions displaced by the flow. As described in Gendrich et al. (1997), and Koochesfahani (1999), such a two-image system offer advantages over the typical single-image system in that no assumption needs to be made *a priori* about the intensity field in a tagged region. For example, one can properly take into account the variations in the initial tagging pattern (e.g. due to laser beam pointing instability, vibration of the optics, non-uniform tracer concentration, etc.), which could otherwise be misinterpreted as flow velocity fluctuations. In our work in liquid-phase flows, we use both non-intensified frame transfer cameras and gated image-intensified detectors, depending on the imaging requirements (e.g. field of view,  $\Delta t$  between image pairs). In gas-phase applications, we use gated image-intensified detectors. See Koochesfahani (1999) for several examples of applications in liquid and gas phase flows. These detectors are all nominally  $512 \times 512$  pixel arrays operating at 30 frame/s. The images are typically digitized to 8 bits by two image acquisition/ processing systems and transferred onto high capacity disk arrays in real time.

Our approach for finding the displacement of tagged regions is based on a direct digital spatial correlation technique, and offers certain advantages over the traditional line-center methods. In particular, it is a more general scheme that is independent of the specific intensity distribution within a tagged region and can accommodate arbitrary tagging patterns including those due to non-uniform scalar mixing fields. The details of this approach and its performance are described in Gendrich & Koochesfahani (1996). Based on both experiments and an extensive statistical study, it has been found that the displacement of the tagged regions can be typically determined with a 95% confidence limit of  $\pm 0.1$  sub-pixel accuracy (i.e. 95% of the displacement measurements are accurate to better than 0.1 pixel). This corresponds to an rms accuracy of  $\pm 0.05$  pixel, assuming a Gaussian distribution for error. For high values of image S/N, the 95% confidence level can be as low as 0.015 pixel (0.0075 pixel rms). An example of the application of this procedure is provided in Figure 1; the velocity vectors shown in this figure are "raw" and have not been filtered or smoothed. Note that the MTV data are typically obtained on an irregularly spaced grid and need to be remapped onto a regular grid in order to take advantage of standard data processing schemes (see Cohn & Koochesfahani, 1999).

It should be mentioned that the combination of two-detector imaging and spatial correlation processing approach allows MTV measurements to be carried out even when the molecular tracer is not uniformly mixed in the working fluid. Currently in our work involving both liquid phase and gas phase flows,  $25 \times 25$  grid patterns are common, resulting in the simultaneous measurement of over 600 independent velocity vectors per plane. In a recent work (Cohn, 1999), between 600 to 800 vectors were measured per plane. The above-mentioned vector density per plane is not limited by the available laser energy (the energy for each tagging beam is in the range 1-2 mJ/pulse

or less), but by the pixel density of our current detector arrays. The velocity measurement density will increase proportionally as denser detector arrays are utilized. The processing of long sequences of MTV image pairs has been automated through a common C algorithm running on both Unix and PC systems. While running on a Silicon Graphics R-10000 (180 MHZ) CPU, the processing speed is about 40 vector/s and about 50% slower when running on a 400-MHZ PentiumII PC. The algorithm has not been optimized for processing speed and improvements are likely. Finally, it should be mentioned that MTV has recently been extended to provide measurement of all three components of the velocity vector over a plane using stereo imaging techniques (Bohl et al. 1999).

## 2. Methods for Simultaneous Velocity-Concentration Measurements

When molecular tagging is used for purely velocimetry, the long-lived molecular tracer is typically homogeneously mixed in the flowing medium (it is either naturally present or premixed in the fluid). As mentioned earlier, however, a homogeneous mixture is not a requirement when using a two-image approach along with the spatial correlation method of processing. The simplest approach for obtaining simultaneous data on velocity and concentration in the mixing between two streams (e.g. a two-stream shear layer or a jet discharging into ambient, etc.) is to premix the tracer in only one stream, as is usually done when using LIF for mixing studies. The intensity field from the first, initially tagged, image is used to infer the scalar concentration in much the same way as in the LIF technique. The velocity field is determined, as before, by correlating the displacement of small regions in the first image with those in the second (delayed) image. Examples of the application of this approach, using the phosphorescent supramolecule tracer, have been given in Koochesfahani et al. (1996) and Gendrich et al. (1997).

The single-tracer approach just described suffers, however, from the deficiency that it is not capable of providing velocity information in the portions of a flow where the tracer concentration is zero, or very small. The regions in a flow where the tracer concentration is high enough for obtaining reliable velocity data is dictated by the scalar mixing field, a property of the dynamics of the flow under investigation. One solution to this problem would be to premix the molecular tracer in both of the mixing stream, but at different free stream concentrations. This method, however, will reduce the dynamic range of the concentration measurements. For a method of most general utility, it is preferable to seek an alternate solution to decouple the measurement of the velocity field from the scalar field measurements. In the next section we describe such a method where two different tracers are used to combine the traditional LIF technique (using fluorescein) with MTV (using phosphorescent supramolecules).

The use of the LIF technique for quantifying the scalar mixing field in water flows is well established and the details of implementation won't be repeated here. The development and application of LIF in non-reacting and reacting flows are described in Koochesfahani & Dimotakis (1985, 1986).

### 3. Development of Experimental Technique

The experiments were performed in a gravity-driven two-stream water shear layer apparatus. The test section has a cross-section of 4 cm (height) x 8 cm (span) and is 35 cm long. The free-stream fluids are supplied from separate reservoirs, and their speeds can be set independently. The facility usually operates with the high-speed stream on the top and the low-speed stream on the bottom. The apparatus has a provision for imposing controlled external perturbations onto the flow. Two-dimensional perturbations can be introduced by oscillating one of the free streams using an oscillating bellows mechanism in one of the supply lines. Further details can be found in Koochesfahani & MacKinnon (1991) and MacKinnon (1999).

For MTV measurements, the phosphorescent triplex compound (1-BrNp • G $\beta$ -CD • ROH) is premixed in the entire flow facility (i.e. both reservoirs). The molar concentrations of the components are  $2 \times 10^{-4}$  M G $\beta$ -CD, 0.06 M cyclohexanol, and a saturated solution of 1-BrNp (approx.  $1 \times 10^{-5}$  M). For LIF measurements, disodium fluorescein is premixed with the reservoir fluid of only one of the free-streams, the lower stream in this study. The free-stream dye concentration is approximately  $2 \times 10^{-7}$  M. A single Lambda-Physik LPX-220i XeCl excimer laser is utilized to both activate the phosphorescence of the triplex compound and excite the fluorescence of fluorescein. This laser generates 20 ns long, 100 mJ, pulses at a wavelength  $\lambda = 308$  nm. The laser beam is converted into a grid of intersecting laser lines, as described earlier, and is used to illuminate the region of interest in the flow.

The schematic in Figure 2 illustrates the experimental setup and the placement of the detectors for the combined MTV-LIF measurements described here. The LIF signal is recorded by a SONY XC-77RR CCD camera (30 frame/s, exposure duration of 1 $\mu$ s) viewing the flow through an orange filter (e.g. filter #15). The MTV image pair is acquired by two Pulnix TM9701 CCD (30 frame/s) cameras viewing a common field of view through a cube beam splitter. The outputs of the three cameras are digitized (8-bits) and transferred to disk in real time using PC-based image acquisition systems. The timing among the three detectors and the pulsed laser is controlled by two digital delay generators (Stanford Research Systems DG535). The general timing diagram is shown in Figure 3, along with the nominal values of the parameters. The fluorescence signal is acquired during the 1 $\mu$ s exposure duration which straddles the laser pulse. The initial image of the tagging

pattern is recorded by the first MTV detector at time  $t = t_o$ , just after the laser fires. As long as this time delay is larger than about 20 ns (actual value used here was 63.5  $\mu$ s), the fluorescence signal will not contaminate the first MTV image since fluorescence is a short-lived excited state, with a lifetime of order nanosecond. The second MTV camera records the later image of the tagged regions at a prescribed time delay  $\Delta t$  after the first detector. For the conditions of the particular experiments discussed here,  $\Delta t$  is about 2 ms and 4 ms for the shear layer and wake experiments, respectively. During this time interval the tagged regions displace a maximum distance of about 8 pixels (nearly 800  $\mu$ m). The sequence described above is repeated at the rate of 30 per second, as dictated by the framing rate of the cameras used.

The potential cross-talk between the MTV and LIF signals is an important issue and is discussed next considering the emission spectra in Figure 4. It is noted in this figure that the fluorescence and phosphorescence emissions of the MTV triplex occur over the approximate wavelength ranges 300-400 nm and 460-700 nm, respectively. The fluorescence emission of fluorescein occurs above wavelengths of about 490 nm. We first consider the effect of the MTV signal on the LIF measurement. During the exposure time of the LIF camera, photons arrive at the camera from four sources: the fluorescence of fluorescein, the fluorescence of MTV triplex, the phosphorescence of the MTV triplex, and spurious scattering of the laser wavelength. Since the laser wavelength and the fluorescence emission of the MTV triplex are spectrally well separated from that of the fluorescein, both can easily be filtered out. We have used an orange filter (photographic filter #15) for this purpose. On the other hand, the quantum efficiency of the triplex phosphorescence is about  $\phi_e = 0.035$ , nearly 1/30th of that for the fluorescein fluorescence (Gendrich et al. 1997). Thus the triplex phosphorescence is easily dominated by the LIF signal. The relatively weak phosphorescence emission, integrated over the exposure period of the LIF camera, would appear as a nearly uniform low-level background in the LIF image, which can be removed during LIF data processing. If needed, this low-level background can be reduced to negligible levels by decreasing the exposure of the LIF detector (1  $\mu$ s in the present case); recall that this exposure period can be lowered to about 20 ns without affecting the recorded fluorescence signal. Two other aspects should also be noted. The triplex is optically transparent to the fluorescence of fluorescein, since the emission spectrum of fluorescein is completely outside the absorption band of the MTV triplex (though not shown, the absorption band of the MTV triplex is known to lie to the left of its fluorescence spectrum in Figure 4). Furthermore, if needed, attenuation of the laser energy due to absorption by the triplex can be properly accounted for with appropriate calibration in a procedure already incorporated in the quantitative processing of LIF images (see Koochesfahani & Dimotakis, 1985).

As for the effect of the LIF signal on MTV measurements, we note that the triplex is only

activated by the primary laser pulse; the fluorescein's emission is not absorbed by the triplex. The MTV image pair (in particular, the first one) is acquired well after the fluorescence emission decays to negligible levels, and, therefore, is not contaminated by the LIF image. For cases where the free-stream fluorescein concentration is high, the absorption of the laser energy by the non-uniform concentration of the scalar mixing field can result in a non-uniform intensity in the grid pattern used for tagging. This aspect poses no difficulties because of the two-detector imaging and the spatial correlation method of processing used for MTV. The absorption of the MTV triplex phosphorescence emission by fluorescein can potentially cause complications in certain unusual circumstances. The issue is akin to the potential self-absorption difficulties that might occur in standard LIF using fluorescein, or any dye whose absorption and emission spectra have an overlap. A small fraction of the light emitted from a tagged region is absorbed by the fluorescein present along the path between the emission site (i.e. the tagged region) and the detector, causing a modification of the luminescence intensity actually recorded by the detector. The extent of this absorption depends on the concentration distribution of fluorescein along the path and the length of the path. If the extent of the absorption for a given tagged region is different at the two time ticks ( $\Delta t$  apart) of the MTV image pair, the luminescence distribution from the tagged region at the two different times will have different "apparent" distributions which can introduce noise in the displacement measurement by the spatial correlation procedure. Should this effect be significant, it will be readily noted by a reduction of the peak value of the correlation coefficient. Such a reduction have not been observed in our work to date. For this artifact to become an issue, the absorption path length has to be not only very long, but the actual distribution of the absorbing species along this path must vary significantly during the brief time interval between the MTV image pair. As a result, we do not expect such complications in most applications.

The discussion above indicates that simultaneous MTV-LIF experiments can be designed with negligible cross-talk between the two diagnostic techniques. A sample of the three-image triad recorded by the three detectors (see Figure 2) for combined MTV-LIF measurements is presented in Figure 5. A relatively low density grid of laser lines (thick-thin combination) was used in this case. The top image shows the concentration field of fluorescein acquired by the LIF camera. The lower two images, acquired by the two MTV cameras, display the initial tagging pattern of the MTV triplex and its subsequent displacement and distortion  $\Delta t$  later. These images are from a turbulent two-stream shear layer for which quantitative data will be presented in the next section.

#### 4. Experimental Results and Discussion

This section provides two examples of the application of the simultaneous MTV-LIF

technique. The first gives an example of the correspondence between a flow pattern obtained from flow visualization and the underlying vorticity field of the flow. The second provides quantitative, simultaneous information on the velocity and scalar mixing field in a turbulent shear layer.

#### ***4.1 Simultaneous Visualization of Flow Pattern and Vorticity Field***

In this experiment, the free stream speeds of the shear layer facility were set to the same value  $U_1 = U_2 \approx 10$  cm/s to generate a wake flow. The wake was forced by oscillating one of the free stream speeds sinusoidally near the Kármán shedding frequency ( $\approx 6$  Hz). Results are shown here for a low and a high forcing amplitude of about 2% and 11.5% rms fluctuation level, respectively. Details of the mixing studies of this flow can be found in MacKinnon & Koochesfahani (1997), and its vorticity dynamics are described in Cohn (1999).

Figure 6(a) depicts examples of simultaneous maps of the spanwise vorticity and visual structure in the forced wake. For completion, the detailed two-component velocity field determined from the regions tagged by the grid pattern is shown in Figure 6(b), along with a traditional LIF visualization of the flow by a laser sheet (Figure 6c). The grid illumination used in this case is more dense than that in Figure 5. Nevertheless, LIF flow visualization with a grid pattern will always have a more "coarse" appearance than that obtained with a laser sheet. It is possible to rectify this by tagging for MTV with one laser and using a second laser for LIF sheet illumination; see Section 5.

Figure 6 shows that at the lower perturbation amplitude (top of Figure 6), two rows of opposite-sign vortex arrays are formed, which are laterally displaced. The peak vorticity levels are relatively low. When the forcing amplitude increases (bottom of Figure 6), the peak vorticity level increases significantly by a factor of more than two, and the lateral displacement of the two rows becomes very small. Simultaneous vorticity-visualization data indicate that, for a high perturbation amplitude, the vorticity contours are centered about the cores of the "jelly-roll" patterns shown by the flow visualization. At low perturbation amplitude, however, the vorticity contours reveal regions of vorticity that are not readily identified by flow visualization alone.

#### ***4.2 Simultaneous Velocity-Concentration Measurements in an Unforced Turbulent Shear Layer***

The free-stream speeds were set to  $U_1 \approx 40$  cm/s and  $U_2 \approx 20$  cm/s for these experiments. The details of the mixing characteristics of this flow are documented in MacKinnon (1999). For the range of downstream distances discussed here, the shear layer is near the end of the mixing transition (Breidenthal, 1981).

We first describe in Figure 7 two typical realizations of the flow structure (revealed by LIF) and its underlying velocity/vorticity field. The LIF images shown are “raw” and have not yet been processed for the extraction of quantitative concentration data. Even though the grid illumination pattern is rather coarse, one can clearly see the passage of two well-separated vortical structures in one example, and the appearance of pairing vortices in the other. The MTV velocity field, along with the corresponding spanwise vorticity, determined from the regions tagged by the grid pattern are shown below each LIF image,. The velocity field is shown in the shear layer convection frame, i.e.  $U_c = (U_1 + U_2)/2$  is subtracted. The unusual diamond-shaped region where the MTV data are shown corresponds to the region containing grid intersections (see Figure 5). The most interesting result from Figure 7 is that the features usually identified as vortical structures in LIF flow visualizations of a mixing layer do, in fact, correspond very well with the underlying vorticity field. In the realization on the left, the MTV data clearly show two well-separated regions of concentrated vorticity and a stagnation point between the two structures. For the realization on the right, two identifiable regions of vorticity are noted in the MTV data in the same spatial arrangement as that in the LIF images.

Quantitative data are presented at a single downstream location  $x = 15.5$  cm in the mid-point of the image plane shown in Figure 7. At this location, the shear layer mean visual thickness is  $\delta_1 \approx 2.5$  cm. Seven individual locations across the shear layer width are selected for the computation of the various mean and fluctuating quantities. The transverse profiles of these quantities will be presented. The scalar concentration field  $\xi$  is extracted from the LIF images using procedures described elsewhere (Koochesfahani & Dimotakis, 1985). Concentration  $\xi$  refers to the high-speed fluid volume fraction and is defined such that  $\xi = 0, 1$  corresponds to pure fluids from the low-speed and high-speed streams, respectively.

Figure 8 summarizes the transverse profiles of all the mean and fluctuating quantities derived from the current simultaneous MTV-LIF measurements. These quantities include the mean streamwise velocity  $U$  and its rms  $u'$ , the transverse velocity rms  $v'$ , the Reynolds stress  $-\overline{u'v'}$ , the average concentration  $\xi_{avg}$  and its rms  $\xi'$  and the velocity-concentration correlations  $\overline{u'\xi'}$  and  $\overline{v'\xi'}$ . The averaging is based on 500 realizations. The velocity information is normalized by  $\Delta U = U_1 - U_2$ , and the transverse coordinate is normalized as  $(y - y_c) / x$ , where  $y_c$  refers to the transverse location where the mean velocity equals the convection speed  $U_c$ .

The mean and fluctuating velocity data in Figure 8 are in good agreement with reported measurements of these quantities. When compared with the data compiled from the shear layer literature (see MacKinnon, 1999), the various measured peak values,  $(u')_{max} / \Delta U = 0.133$ ,  $(v')_{max} / \Delta U = 0.157$ , and  $(-\overline{u'v'})_{max} / (\Delta U)^2 = 0.0082$ , fit very well for the shear layer Reynolds number under investigation here. The average concentration profile exhibits the typical shape,

characterized by three inflection points, observed in previous passive scalar measurements (e.g. Fiedler, 1974; Brown & Roshko, 1974; Koochesfahani & Dimotakis, 1985; MacKinnon & Koochesfahani, 1991). The rms concentration profile shows a double-peaked structure similar to that previously observed by Wygnanski et al. (1979) in mixing layer temperature measurements. The peak value of passive scalar concentration rms in Figure 8 is also comparable to that reported by Wygnanski et al. (1979).

The transverse profiles of velocity-concentration correlations show some interesting features. Note that  $\overline{u'\xi'}$  has nearly a bell-shaped profile, whereas  $-\overline{v'\xi'}$  remains fairly constant over a large region in the middle of the mixing layer. This result implies that a turbulent mass diffusion coefficient  $D_T$ , defined in a gradient diffusion model as  $-\overline{v'\xi'} = D_T \partial(\xi_{avg})/\partial y$ , would not be a constant in the plane mixing layer. We are not aware of such velocity-concentration data for plane mixing layers in the literature and, therefore, quantitative comparisons with existing data cannot be made.

## 5. Concluding Remarks

The approach described in this paper uses a single laser and two tracers to combine MTV with LIF for the purpose of simultaneous velocity-concentration measurements. A phosphorescent triplex compound is used for MTV, along with fluorescein for LIF in applications involving liquid-phase flows. This approach can be extended to accommodate caged-fluorescein as the MTV tracer, and is also applicable to tracers for gas-phase flows.

An aspect requiring a consideration is the fact that such "simultaneous" measurements are, in fact, not exactly simultaneous. There is a temporal shift between the LIF image and when the velocity data are available (at the mid-point of the MTV image pair). This issue arises in all time-of-flight velocimetry techniques such as PIV and MTV. It is currently difficult for these whole-field imaging techniques to provide the velocity data rates necessary to resample the velocity at the time of LIF image. One way to minimize the potential artifacts connected to the temporal shift is to obtain the LIF image at the mid-point of the MTV image pair. This, however, would sacrifice the simplicity of a single-laser system in favor of a second laser for LIF imaging. The lasers typically in use for LIF using laser dyes such as fluorescein (i.e. argon-ion at 488 nm and 514.5 nm, or YAG at 532 nm) can be integrated into the system we have described here. The wavelengths of these lasers do not fall within the absorption band of the MTV triplex and, therefore, will not interfere with velocity measurements. An added benefit would be that a laser sheet can now be used for the usual planar LIF imaging instead of the coarser images provided by a grid pattern of illumination.

## Acknowledgments

This work was supported by the MRSEC Program of the National Science Foundation, Award Numbers DMR-9400417, and DMR-9809688. We gratefully acknowledge the additional support by the Palace Knight Program of the United States Air Force Research Laboratory.

## References

Bohl, D. G., Koochesfahani, M. M., and Olson, B. J. [1999] "Development of stereoscopic molecular tagging velocimetry." Submitted to *Exp. Fluids*.

Breidenthal, R. E. [1981] "Structure in turbulent mixing layers and wakes using a chemical reaction." *J. Fluid Mech.*, Vol. 109, 1-24.

Brown, G. L. & Roshko, A. [1974] "On density effects and large structure in turbulent mixing layers." *J. Fluid Mech.*, Vol. 64, Pt. 4, 775-816.

Chevray, R. & Tutu, N. K. [1978] "Intermittency and preferential transport of heat in a round jet." *J. Fluid Mech.*, Vol. 88, 133-160.

Cohn, R. K. [1999] "Effect of forcing on the vorticity field in a confined wake," PhD thesis, Michigan State University.

Cohn, R. K. and Koochesfahani, M. M. [1999] "The accuracy of remapping irregularly spaced velocity data onto a regular grid and the computation of vorticity," *Proceedings of the 3rd International Workshop on PIV*, Ed. Adrian, R., Hassan, Y, and Meinhart, C., 225-230; submitted to *Exp. Fluids*.

Cowen, E. A. and Chang, K. A. [1999] "A single camera coupled PTV-LIF technique." Proceedings of The Third International Workshop on PIV'99, Eds. R. Adrian, Y. Hassan, C. Meinhart; Santa Barbara, CA, Sept. 16-18, 1999, 371-378.

Dabiri, D. & Gharib, M. [1996] "The effects of forced boundary conditions on flow within a cubic cavity using digital particle image thermometry and velocimetry (DPITV)," *Experimental Thermal and Fluid Science*, Vol.13, No. 4, 349-363.

Dahm, W. J. A., Su, L. K., and Southerland, K. B. [1992] "A scalar imaging velocimetry technique for fully resolved four-dimensional vector velocity field measurements in turbulent flows." *Phys. Fluids A*, Vol. 4, No. 10, 2191-2206.

Dibble, R. W. & Schefer, R. W. [1983] "Simultaneous measurement of velocity and scalars in a turbulent non-premixed flame by combined laser Doppler velocimetry and laser Raman scattering." *Turbulent Shear Flows 4: 4th Int. Symp. Turbulent Shear Flows, Karlsruhe, Germany, September 12-14*, pp. 319-327.

Falco, R. E. and Chu, C. C. [1987] "Measurement of two-dimensional fluid dynamic quantities using a photochromic grid tracing technique." *SPIE*, Vol. 814, 706-710.

Falco, R. E. and Nocera, D. G. [1993] "Quantitative multipoint measurements and visualization of dense solid-liquid flows using laser induced photochemical anemometry (LIPA), in *Particulate Two-Phase Flow*, Ed. M. C. Rocco; Butterworth-Heinemann, 59-126.

Fiedler, H. E. [1974] "Transport of heat across a plane turbulent mixing layer," *Advances in Geophysics*, Vol. 18A, 93-109.

Frank, J. H., Lyons, K. M. & Long, M. B. [1996] "Simultaneous scalar / velocity field measurements in turbulent gas-phase flows." *Combustion and Flame*, Vol. 107, 1-12.

Gendrich, C. P. and Koochesfahani, M. M. [1996] "A spatial correlation technique for estimating velocity fields using Molecular Tagging Velocimetry (MTV)." *Exp. Fluids*, Vol. 22, No. 1, 67-77.

Gendrich, C. P., Koochesfahani, M. M. & Nocera, D. G. [1997] "Molecular tagging velocimetry and other novel applications of a new phosphorescent supramolecule." *Exp. Fluids*, Vol. 23, 361-372.

Grissino, A. S., Hart, D. P., and Lai, W. T. [1999] "Combined dual emission LIF and PIV to resolve temperature and velocity." Proceedings of the 3<sup>rd</sup> International Workshop on PIV'99, Eds. R. Adrian, Y. Hassan, C. Meinhart; Santa Barbara, CA, Sept. 16-18, 1999, 591-597.

Hartmann, W. K., Gray, M. H. B., Ponce, A., and Nocera, D. G. [1996] "Substrate induced phosphorescence from cyclodextrin · lumophore host-guest complexes." *Inorg. Chim. Acta*, Vol. 243, 239.

Hishida, K. & Sakakibara, J. [1999] "Combined PLIF-PIV technique for velocity/scalar fields." Proceedings of the 3<sup>rd</sup> International Workshop on PIV'99, Eds. R. Adrian, Y. Hassan, C. Meinhart; Santa Barbara, CA, Sept. 16-18, 1999, 21-30.

Keagy, W. R. & Weller, A. E. (1949), "A study of freely expanding inhomogeneous jets." *Proc. Heat Transf. Fluid Mech. Inst.*, Vol. 1-3, 89-98.

Koochesfahani, M. M., Cohn, R. K., Gendrich, C.P. & Nocera, D .G. [1996] "Molecular tagging diagnostics for the study of kinematics and mixing in liquid phase flows." Proceedings of the *Eight International Symposium on Applications of Laser Techniques to Fluids Mechanics*, July 8 - 11, 1996, Lisbon, Portugal, vol. I, 1.2.1-1.2.12; Also in **Developments in Laser Techniques and Fluid Mechanics**, Chapter 2, section 1, Eds. Adrian, Durao, Durst, Maeda, and Whitelaw; Springer-Verlag., 1997.

Koochesfahani, M. M. & Dimotakis, P. E. [1985] "Laser induced fluorescence measurements of mixed fluid concentration in a liquid plane shear layer." *AIAA J.*, Vol. 23, No. 11, 1700-1707.

Koochesfahani, M. M. & Dimotakis, P. E. [1986] "Mixing and chemical reactions in a turbulent liquid mixing layer." *J. Fluid Mech.*, Vol. 170, 83-112.

Koochesfahani, M. M. & MacKinnon, C. G. [1991] "Influence of forcing on the composition of mixed fluid in a two-stream shear layer." *Phys. Fluids A*, Vol 3, No. 5, 1135-1142.

Koochesfahani, M. M. & MacKinnon, C. G. [1998a] "Methods for simultaneous velocity/pассив scalar measurements using molecular tagging diagnostics." Proceedings of the 13<sup>th</sup> U.S. National Congress of Applied Mechanics, June 21-26, 1998, Gainesville, Florida, MA2.

Koochesfahani, M. M. & MacKinnon, C. G. [1998b] "Simultaneous velocity/pассив scalar measurements using a molecular tagging technique." *Bull. Am. Phys. Soc.*, Vol. 43, No. 9, 1989.

Koochesfahani, M. M. [1999] "Molecular tagging velocimetry (MTV): Progress and Applications." AIAA Paper No. AIAA-99-3786.

Law, A.W.K., and Wang, H. [1999] "Simultaneous velocity and scalar field measurements of axisymmetric plumes with combined DPIV and PLIF." Proceedings of the 3<sup>rd</sup> International Workshop on PIV'99, Eds. R. Adrian, Y. Hassan, C. Meinhart; Santa Barbara, CA, Sept. 16-18, 1999, 445-450.

Lemoine, F., Wolff, M. & Lebouche, M. [1996] "Simultaneous concentration and velocity measurements using combined laser-induced fluorescence and laser Doppler velocimetry: Application to turbulent transport." *Exp. Fluids*, Vol. 20, 319-327.

Lempert, W. R., Magee, K., Ronney, P., Gee, K. R., and Haughland, R. P. [1995] "Flow tagging

velocimetry in incompressible flow using photo-activated nonintrusive tracking of molecular motion (PHANTOMM)." *Exp. Fluids*, Vol. 18, 249-257.

Maas, H.G., Stefanidis, A., and Gruen, A. [1994] "Feature tracking in 3-D fluid tomography sequences." First IEEE International Conference on Image Processing, Austin, Texas, November 13-16, 1994.

MacKinnon, C. G. and Koochesfahani, M. M. [1997] "Flow structure and mixing in a low Reynolds number forced wake inside a confined channel." *Phys. Fluids*, Vol. 9, No. 10, 3099-3101.

MacKinnon, C. G. [1999] "Effects of 2-D and 3-D forcing on molecular mixing in a two-stream shear layer." PhD thesis, Michigan State University.

Miles, R., Cohen, C., Connors, J., Howard, P., Huang, S., Markovitz, E., and Russell, G. [1987] "Velocity measurements by vibrational tagging and fluorescent probing of oxygen." *Optics Letters*, Vol. 12, No. 11, 861-863.

Miles, R. B., Connors, J. J., Markovitz, E. C., Howard, P. J., and Roth, G. J. [1989] "Instantaneous profiles and turbulence statistics of supersonic free shear layers by Raman Excitation plus Laser-Induced Electronic Fluorescence (RELIEF) velocity tagging of oxygen." *Exp. Fluids*, Vol. 8, 17-24.

O'Hern, T. J., Tieszen, S. R., Gerhart, A. L., Schefer, R. W., Young, C. and Weckman, E. J. [1999] "Simultaneous measurement of velocity and concentration fields using a high-speed motion picture PIV/LIF system in a buoyant helium plume." Proceedings of the 3<sup>rd</sup> International Workshop on PIV'99, Eds. R. Adrian, Y. Hassan, C. Meinhart; Santa Barbara, CA, Sept. 16-18, 1999, 585-590.

Owen, F. K. [1976] "Simultaneous laser measurements of instantaneous velocity and concentration in turbulent mixing flows." *Proc. AGARD Conf. On Applications of Non-Intrusive Instrumentation in Fluid Flow Research, AGARD-CP-193*.

Ozawa, M., Müller, U., Kimura, I., and Takamori, T. [1992] "Flow and temperature measurement of natural convection in a Hele-Shaw cell using a thermo-sensitive liquid-crystal tracer." *Exp. Fluids*, Vol. 12, 213-222.

Pearlstein, A. J. and Carpenter, B. N. [1995] "On the determination of solenoidal or compressible velocity fields from measurements of passive or reactive scalars." *Phys. Fluids*, Vol. 7, No. 4, 754-763.

Pitz, R. W., Brown, T. M., Nandula, S. P., Skaggs, P. A., DeBarber, P. A., Brown, M. S., and Segall, J. [1996] "Unseeded velocity measurement by ozone tagging velocimetry." *Optics Letters*, Vol. 21, No. 10, 755-757.

Ribarov, L. A., Wehrmeyer, J. A., Batliwala, F., Pitz, R. W., and DeBarber, P. A. [1999] "Ozone tagging velocimetry using narrowband excimer lasers." *AIAA J.*, Vol. 37, No. 6, 708-714.

Ponce, A., Wong, P. A., Way, J. J. & Nocera, D. G. [1993] "Intense phosphorescence triggered by alcohols upon formation of a cyclodextrin ternary complex." *J. Phys. Chem.*, Vol. 97, 11137-11142.

Popovich, A. T. and Hummel, R. L. [1967] "A new method for non-disturbing turbulent flow measurement very close to a wall." *Chem. Eng. Soc.*, Vol. 22, 21-25.

Stärner, S. H. [1983] "Joint measurement of radial velocity and scalars in a turbulent diffusion flame." *Combust. Sci. Technol.*, Vol. 30, 145-169.

Stier, B. and Koochesfahani, M. M. [1999] "Molecular tagging velocimetry (MTV) measurements in gas phase flows." *Exp. Fluids*, Vol. 26, No. 4, 297-304.

Tokumaru, P. T. and Dimotakis, P. E. [1995] "Image correlation velocimetry." *Exp. Fluids*, Vol. 19,

1-15.

Way, J. & Libby, P. A. [1970] "Hot-wire probes for measuring velocity and concentration in helium and air mixture." *AIAA J.*, Vol. 8, 976-978.

Way, J. & Libby, P. A. [1971] "Application of hot-wire anemometry and digital techniques to measurements in a turbulent helium jet." *AIAA J.*, Vol. 9, 1567-1573.

Webster, D. R., Roberts, P. J. W., and Ra'ad, L. [1999] "Simultaneous DPTV/LIF measurements of a turbulent jet." Proceedings of the 3<sup>rd</sup> International Workshop on PIV'99, Eds. R. Adrian, Y. Hassan, C. Meinhart; Santa Barbara, CA, Sept. 16-18, 1999, 599-605.

Wehrmeyer, J. A., Ribarov, L. A., Oguss, D. A., and Pitz, R. W. [1999] "Flame flow tagging velocimetry with 193 nm H<sub>2</sub>O photodissociation." *Applied Optics*, Vol. 38, No. 33, 6912-6917.

Wygnanski, I., Oster, D., Fiedler, H. [1979] "A forced, plane, turbulent mixing layer: A challenge for the predictor." **Turbulent Shear Flows 2**, 2<sup>nd</sup> International Symposium on Turbulent Shear Flows, July 2-4, 1979, Springer 1980, 314-326.

## List of Figures

Figure 1. Typical MTV image pairs and the resultant 2-component velocity vector field (Gendrich et al. 1997). The flow shown is from a vortex ring impacting a flat wall at normal incidence. The axis of symmetry is indicated by the dashed lines. (a) grid imaged 1  $\mu$ s after the laser pulse; (b) same grid imaged 8ms later; (c) velocity field derived from (a) and (b).

Figure 2. Experimental set-up for combined MTV-LIF measurements.

Figure 3. Timing diagram for combined MTV-LIF measurements.

Figure 4. (a) Fluorescence and phosphorescence emission of MTV triplex compound (A: without alcohol; B: with alcohol), and (b) fluorescence emission of fluorescein.

Figure 5. Sample images for simultaneous concentration/velocity measurements.

Figure 6. Results in a forced wake: (a) simultaneous flow visualization and vorticity data (contours at  $\pm 4, 6, 10, 14, 18, \dots, s^{-1}$ ), (b) velocity field (in vortex convection frame) and vorticity field, (c) traditional LIF visualization with a laser sheet.

Figure 7. Two realizations of simultaneous velocity-concentration measurements in a turbulent two-stream shear layer. LIF image (not processed) is on top, and velocity/vorticity fields from MTV are on the bottom. Vorticity is shown in flooded contours and velocity field is in the shear layer convection frame.

Figure 8. Velocity and concentration data in a turbulent two-stream shear layer using simultaneous MTV-LIF measurements.

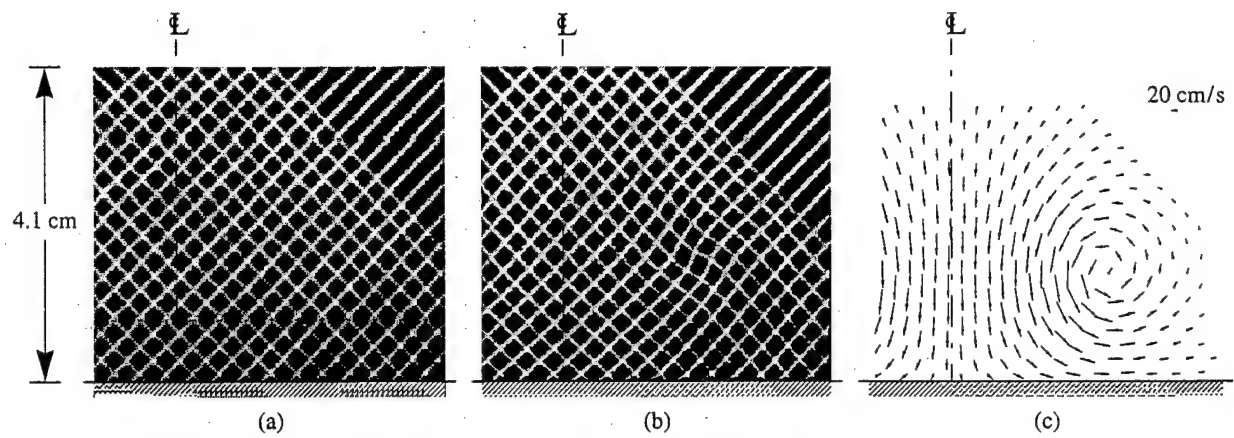
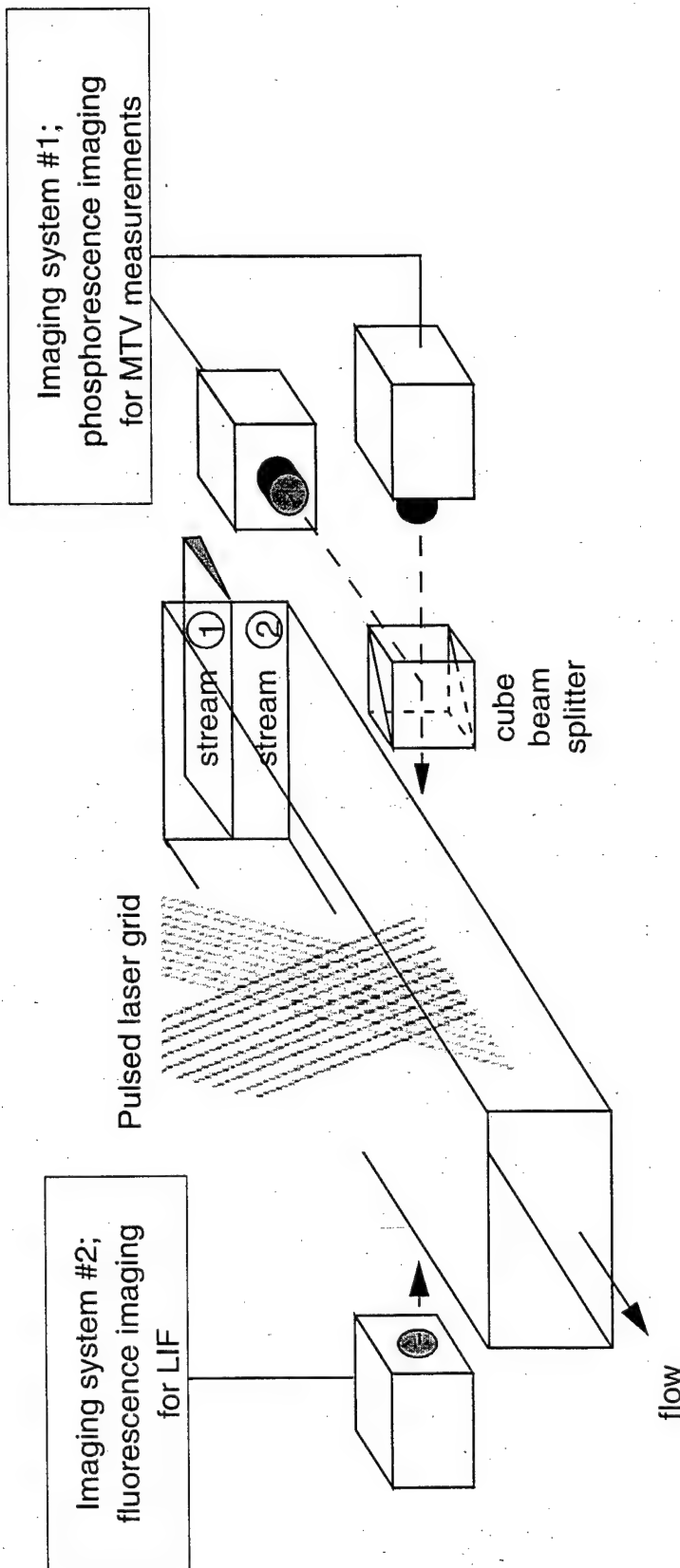


Figure 1. Typical MTV image pairs and the resultant 2-component velocity vector field (Gendrich et al. 1997). The flow shown is from a vortex ring impacting a flat wall at normal incidence. The axis of symmetry is indicated by the dashed lines. (a) grid imaged  $1\mu\text{s}$  after the laser pulse; (b) same grid imaged 8ms later; (c) velocity field derived from (a) and (b).



Stream 1 contains triplex phosphorescent compound  
Stream 2 contains triplex phosphorescent compound + fluorescein

Figure 2. Experimental set-up for combined MTV-LIF measurements.

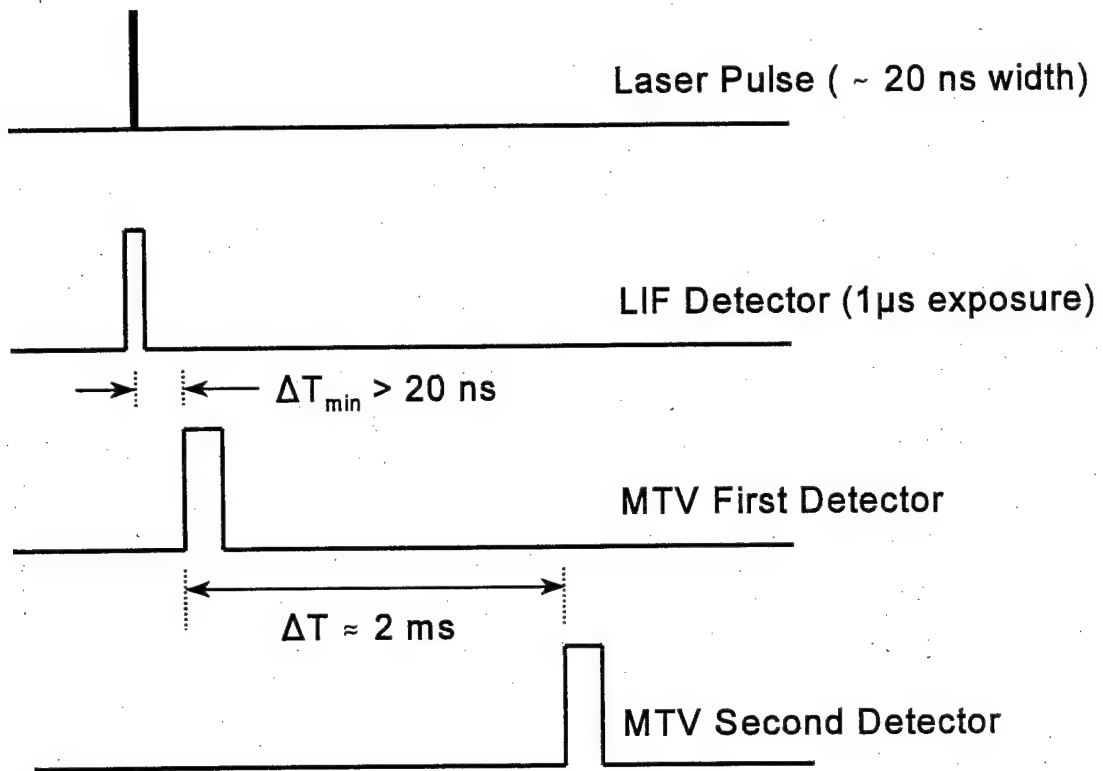


Figure 3. Timing diagram for combined MTV-LIF measurements.

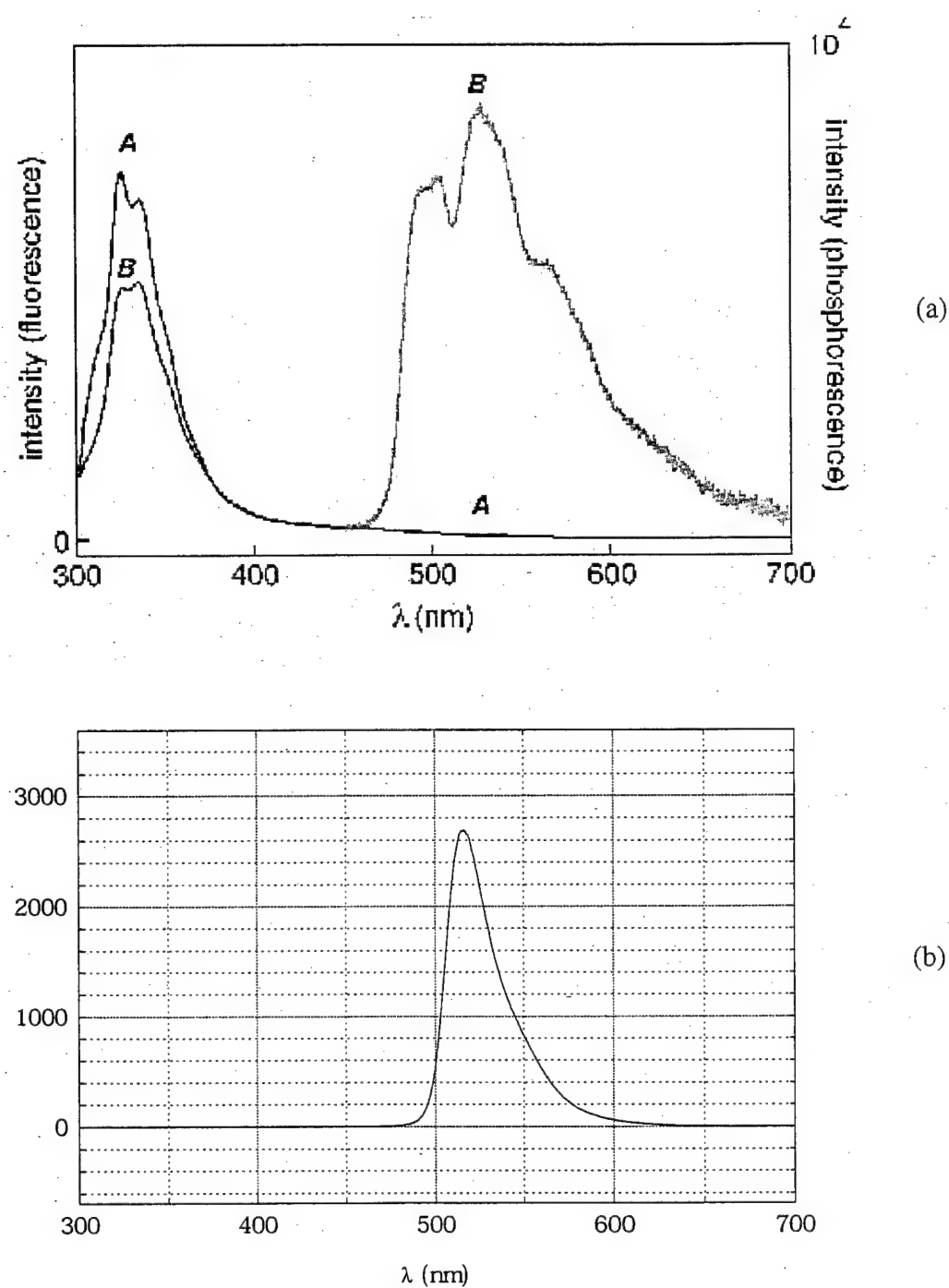
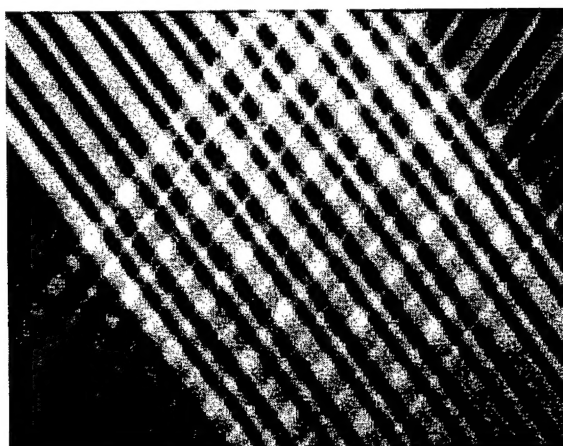


Figure 4. (a) Fluorescence and phosphorescence emission of MTV triplex compound (A: without alcohol; B: with alcohol), and (b) fluorescence emission of fluorescein.

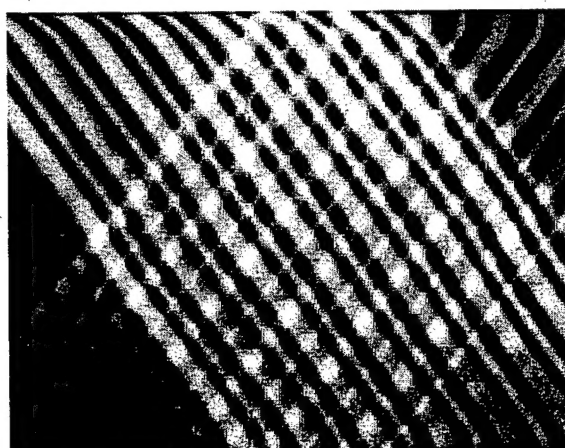


LIF Image



MTV Image Pair

MTV: Image of tagged regions  
at  $t = t_0$ .



MTV: Image of tagged regions  
at  $t = t_0 + \Delta t$ .

Figure 5. Sample images for simultaneous concentration/velocity measurements.

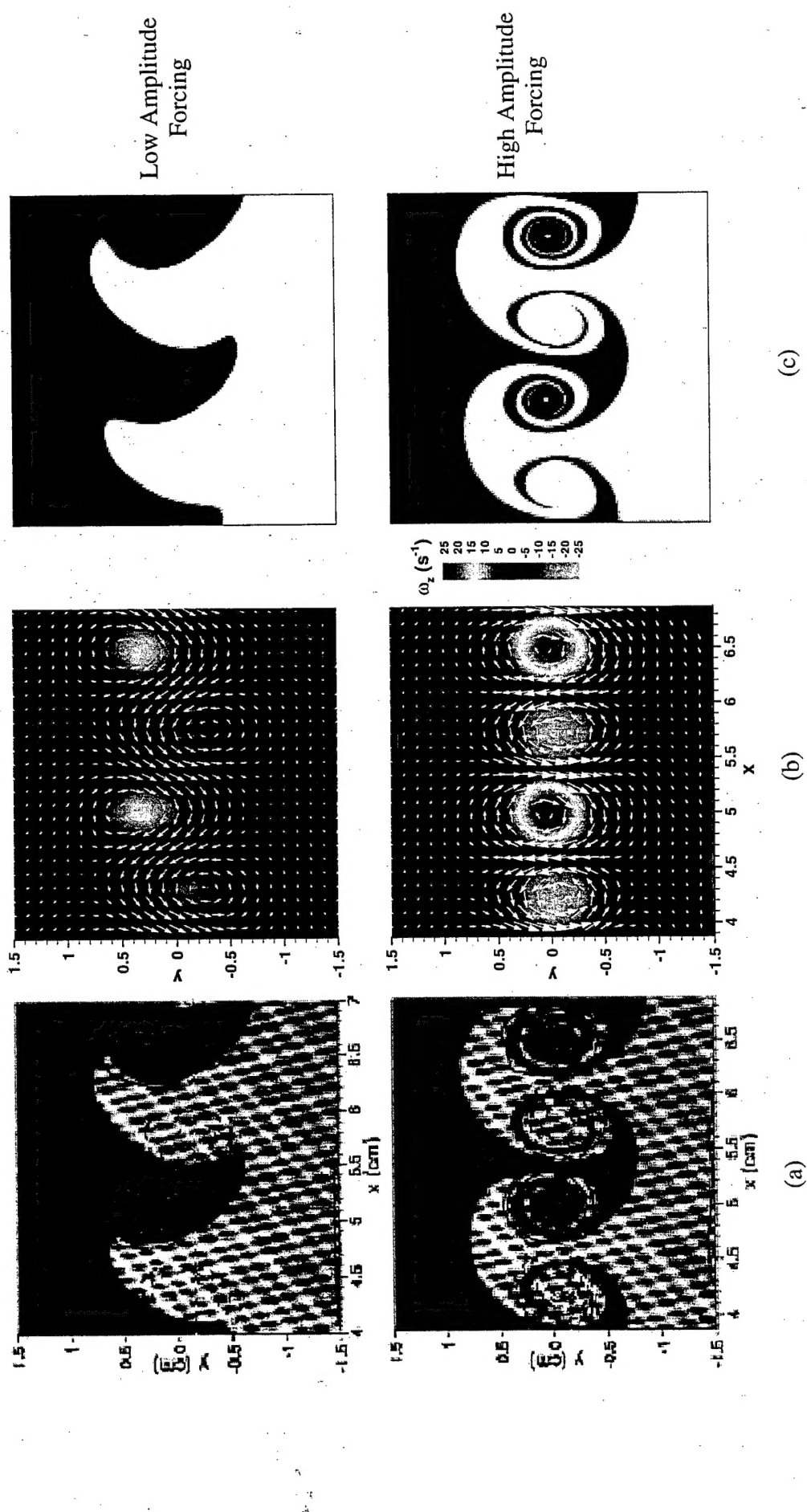


Figure 6. Results in a forced wake: (a) simultaneous flow visualization and vorticity data (contours at  $\pm 4, 6, 10, 14, 18, \dots, \text{s}^{-1}$ ), (b) velocity field (in vortex convection frame) and vorticity field, (c) traditional LIF visualization with a laser sheet.

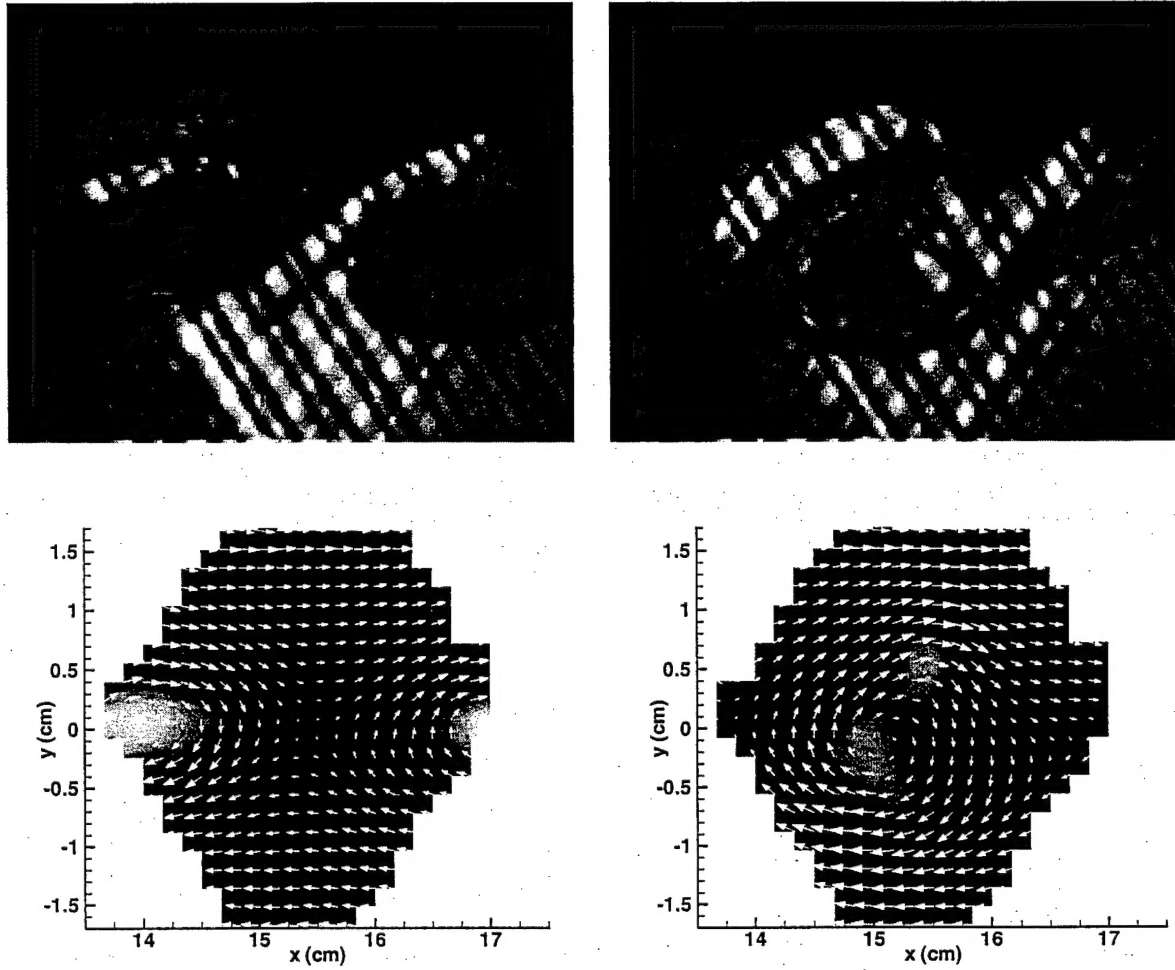


Figure 7. Two realizations of simultaneous velocity-concentration measurements in a turbulent two-stream shear layer. LIF image (not processed) is on top, and velocity/vorticity fields from MTV are on the bottom. Vorticity is shown in flooded contours and velocity field is in the shear layer convection frame.

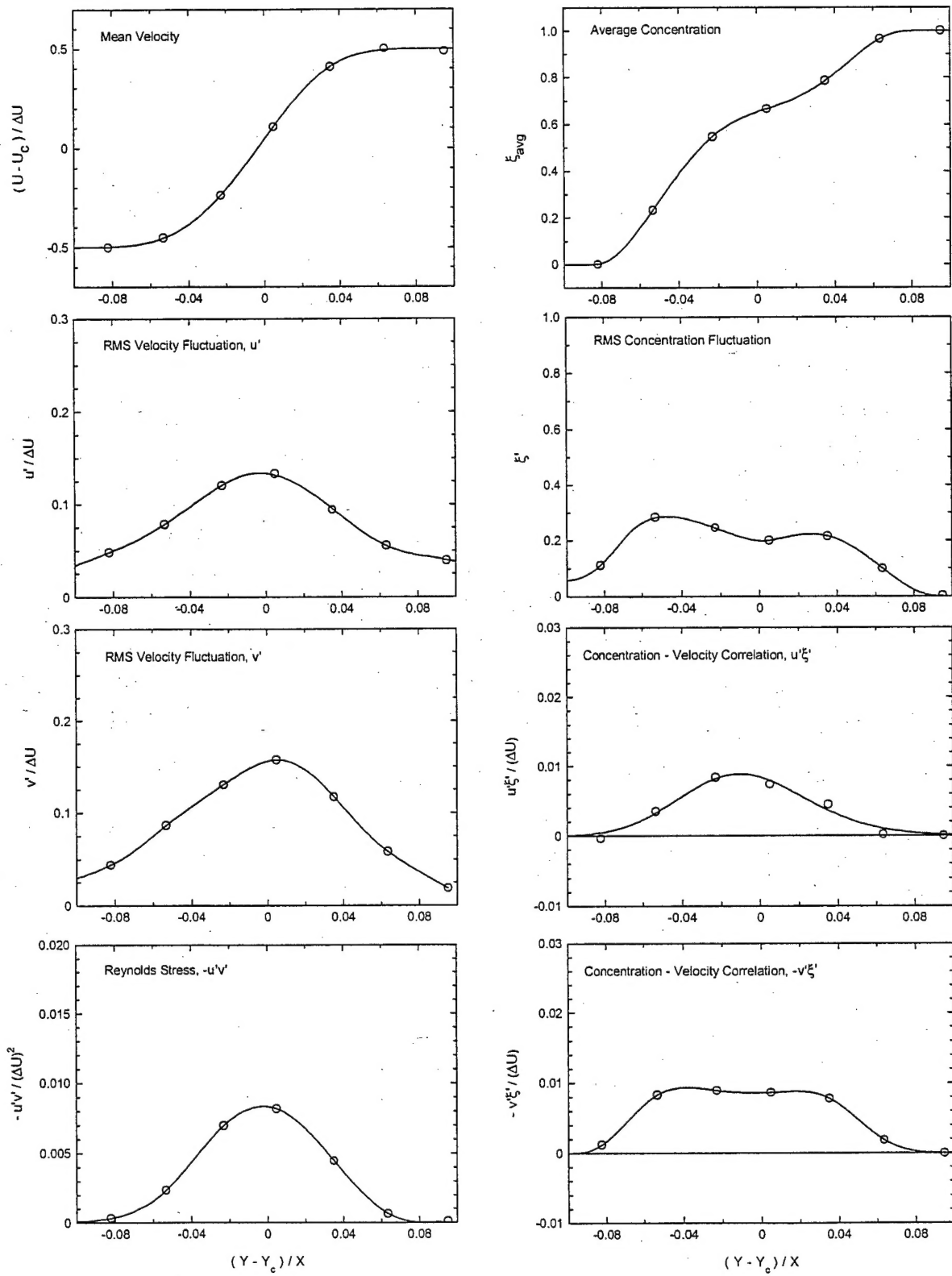


Figure 8: Velocity and concentration data in a turbulent two-stream shear layer using simultaneous MTV-LIF measurements.